

Synthesis of tin oxide nanoparticles by sol–gel process: effect of solvents on the optical properties

S. Gnanam · V. Rajendran

Received: 25 August 2009 / Accepted: 7 December 2009 / Published online: 22 December 2009
© Springer Science+Business Media, LLC 2009

Abstract Tin oxide (SnO_2) nanoparticles were synthesized by the reaction of $\text{SnCl}_4 \cdot 5\text{H}_2\text{O}$ in methanol, ethanol and water via sol–gel method. The samples were characterized by X-ray diffraction (XRD), Fourier transform infrared, Scanning electron microscopy and Transmission electron microscopy. The optical properties of the as-prepared samples were investigated. The XRD analysis showed well crystallized tetragonal SnO_2 can be obtained and the crystal sizes were 3.9, 4.5 and 5 nm for the sample calcined at 400 °C for 2 h. It was found that solvents played important roles in the particle size effect of nanocrystalline SnO_2 .

Keywords Semiconductors · Nanoparticles · Tin oxide · Sol–gel method · Optical properties

1 Introduction

Great efforts have been devoted to synthesize nanoparticles of semiconductors, owing to their fascinating electronic, catalytic and optical properties, which lead to their potential applications as light-emitting diodes [1], catalysts and solar cells [2]. Tin oxide (SnO_2), with a rutile-type crystalline structure, is an n-type wide band gap (3.6 eV) semiconductor that presents a proper combination of chemical, electronic and optical properties that make it advantageous in several applications [3]. Due to its physical properties, such as transparency and semi conductivity,

it is an oxide of great interest from the technological point of view for gas sensors [4], white pigments for conducting coatings, transparent conducting coatings for furnaces and electrodes [5], opto-conducting coatings for solar cells [6], catalysts [7, 8] and surge arrestors (varistors) [9, 10]; an increasing interest in the use of anodes of SnO_2 in lithium batteries has been recently noticed [11]. Nanostructured SnO_2 particles have been prepared by using different chemical methods such as precipitation, hydrothermal, sol–gel, gel-combustion and spray pyrolysis [12–19]. Among various chemical synthesis methods for preparation of metal oxides of large surface area, a sol–gel process offers several advantages over other methods, better homogeneity, controlled stoichiometry, high-purity, phase-pure powders at a lower temperature and flexibility of forming dense monoliths, thin films or nanoparticles.

In general, the band gap increases with the decrease of particle sizes if the particle size is lower than the critical size (which forms excitons in semiconductor). Else, only surface effect could be observed on those particles with size greater than the critical size. The particles with size lower than the critical size can be considered as quantum particles or quantum dots, which exhibit intermediate behavior between molecule or atomic clusters and conventional crystal [20, 21]. The PL spectra of nanostructured materials are usually broad and often asymmetric. Study of particle size with PL of nanocrystalline SnO_2 has been progressed despite different views. As particle size decreases, surface to volume ratio increases and more traps (holes or electrons or excitons) are developed in smaller particles. The physical state of tin oxide nanocrystalline, e.g., the grain size and morphology, is very important on its electronic and optical properties. The gas sensitivity, for example, increases sharply with the decrease of the diameter of tin oxide below a critical value (6 nm) [22].

S. Gnanam (✉) · V. Rajendran
Department of Physics, Presidency College, Chennai, Tamilnadu
600 005, India
e-mail: gn_1984@yahoo.com; gnanam.sambatham@gmail.com

The main purpose of the present research is to study the influence of solvents on the size, morphology and hence, optical properties of the synthesized nanomaterials were investigated.

2 Experimental procedure

All chemical reagents were commercial with AR purity, and used directly without further purification. In a typical synthesis, a transparent sol solution was prepared by dissolving 3.5 g of tin tetrachloride pentahydrate ($\text{SnCl}_4 \cdot 5\text{H}_2\text{O}$) in 100 mL methanol (CH_3OH) under vigorous stirring. 4 mL of an aqueous ammonia solution was added to the above solution by drop wise under stirring. The dropping rate must be well controlled for the chemical homogeneity. The resulting opal gels were filtered and washed with methanol to remove impurities, and dried over 80 °C for 5 h in order to remove water molecules. Finally, ash colored tin oxide nanopowders were formed at 400 °C for 2 h. The same procedure was followed for the preparation of tin oxide nanoparticles using ethanol and water as a solvent.

The XRD pattern of the SnO_2 powder was recorded by using a powder X-ray diffractometer (Schimadzu model: XRD 6000 using $\text{CuK}\alpha$ ($\lambda = 0.154$ nm) radiation, with a diffraction angle between 20 and 80 °. The crystallite size was determined from the broadenings of corresponding X-ray spectral peaks by using Debye–Scherrer's formula. The Fourier transform infrared (FTIR) spectra of the samples were taken using a FTIR model Bruker IFS 66 W Spectrometer. UV–Vis absorption spectra for the samples recorded using a Varian Cary 5E spectrophotometer in the range of 200–800 nm for the powder samples (calcined at 400 °C) in Nujol mode. The photoluminescence (PL) spectra of the SnO_2 were recorded by Perkin-Elmer lambda 900 spectrophotometer with a Xe lamp as the excitation light source. Scanning Electron Microscopy (SEM) studies were carried out on JEOL, JSM- 67001. Transmission electron microscope (TEM) images were taken using an H-800 TEM (Hitachi, Japan) with an accelerating voltage of 100 kV.

3 Results and discussion

Figure 1 shows the XRD patterns of the as-prepared SnO_2 nanoparticles calcined at 400 °C for 2 h using methanol, ethanol and water as a solvent. All samples present wide diffraction peaks at the same position, which can be indexed to the tetragonal rutile structure of SnO_2 (JCPDS card no.88-0287). The XRD pattern of the organic mediated sample (Fig. 1a, b) shows slight broadening of peaks compared to that of the aqueous mediated sample (Fig. 1c).

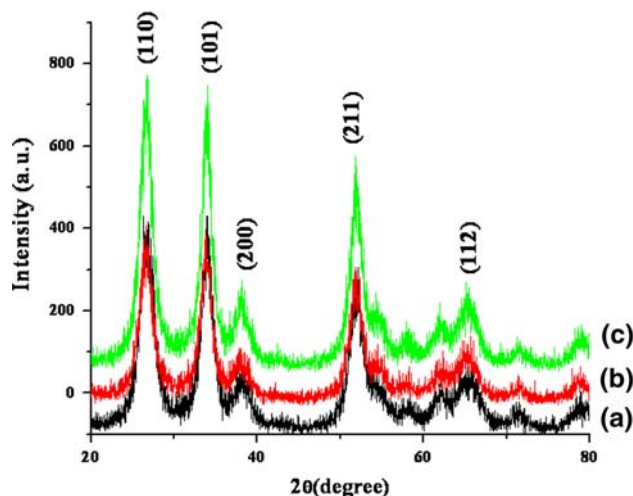


Fig. 1 XRD pattern of SnO_2 nanoparticles mediated in methanol (a), ethanol (b), and water (c)

Using Scherer's formula the average crystallite sizes of the SnO_2 nanocrystals obtained from methanol, ethanol and water were found to be 3.9, 4.5 and 5 nm, respectively. From the results, the methanol mediated SnO_2 nanoparticles were most ultra-fine owing to best dispersing and capping ability.

The FTIR spectrum of as-synthesized SnO_2 dried at 80 °C is shown in Fig. 2a. The broad envelop in the higher energy region about $3,500\text{ cm}^{-1}$ is due to $-\text{OH}$ vibration of methanol and that of water absorbed on the SnO_2 particle surface. Presence of alcohol is also evident by its C–H stretching vibration just below $3,500\text{ cm}^{-1}$ and it is bending vibration at about $1,450\text{ cm}^{-1}$. The CH_3-O

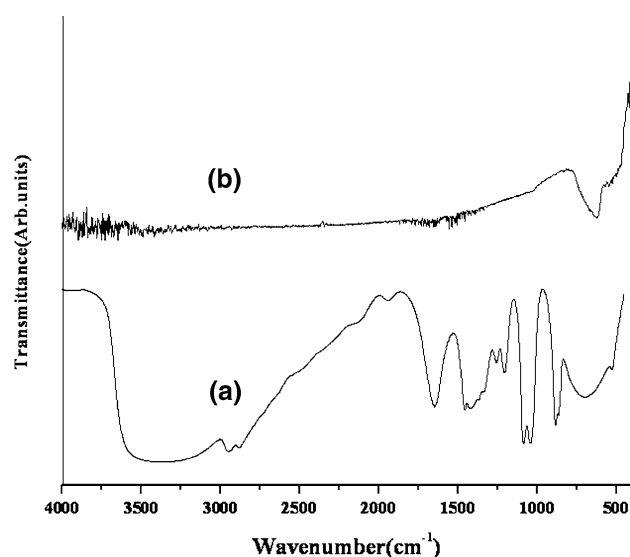


Fig. 2 FTIR spectra of SnO_2 nanoparticles mediated in methanol a 80 °C and b 400 °C

vibration of methanol gives a sharp intense peak at about $1,010\text{ cm}^{-1}$. Presence of water is also evident by its sharp peak at about $1,630\text{ cm}^{-1}$. The broadband in the lower energy region is assigned to Sn–O vibration. Hence, methanol as well as water might control the size of SnO₂ during the synthesis. The FTIR spectrum of SnO₂ calcined at 400 °C is shown in Fig. 2b. As the broadband in the higher energy region in Fig. 2a is completely lost in the spectrum, both CH₃–O and –OH are expelled during calcination. However, the peak at 602 cm^{-1} is assigned to SnO₂ vibration, which indicates that the products are well crystallized.

Figure 3 shows the SEM morphology of tin oxide nanoparticles derived from methanol, an opal gel calcined at 400 °C for 2 h. It shows a spherical morphology of the prepared SnO₂ nanoparticles. This is because methanol functions as a spacer to modulate distance between metal ions preventing metal oxide particles from aggregation during earlier stages of organics removal. Therefore, we can conclude that the observed particles in these SEM images were primary particles. In this preparation method, the gel structure was maintained during the rutile SnO₂ nanoparticles formation process. The powders are found to be fine and slightly agglomerated.

The morphologies and particle sizes were further investigated by TEM. Figure 4 shows the TEM images of the as-prepared SnO₂ nanoparticles calcined at 400 °C using methanol, ethanol and water as a solvent. The obvious rings of selective area electron diffraction (SAED) in the inset of Fig. 4 indicate that all the products are polycrystalline. Figure 4a shows methanol mediated SnO₂ nanoparticles with spherical morphology of size about 3 nm. Most of the nanoparticles were well separated although some of them partially aggregated. The size of the

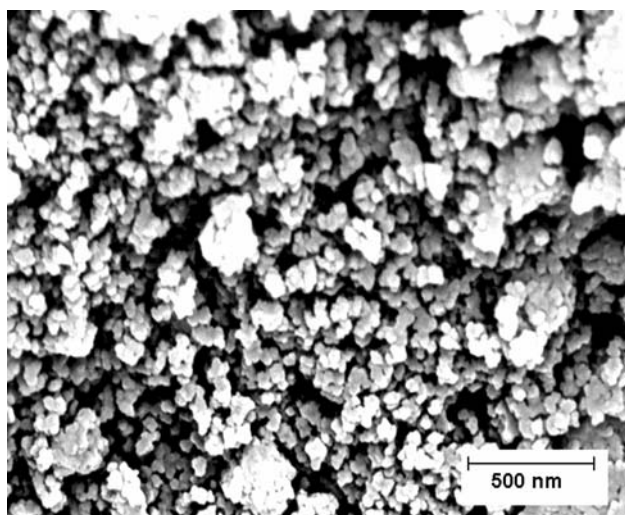


Fig. 3 SEM image of the as-prepared SnO₂ nanoparticles

nanocrystallites is comparable to the Bohr radius (2.7 nm) of SnO₂ and is similar to that calculated from Scherrer's equation. Figure 4b, c reveals TEM pattern of sample prepared in ethanol and water. Comparing to that of methanol, slightly elongate nanoparticles of SnO₂ nanocrystallites were obtained and the size of the products were increased to ca. 4.5 and 5 nm. Moreover, the particle sizes of all the samples obtained from TEM patterns are quite similar to those calculated from Scherrer's equation. Figure 4d, e and f shows the high-resolution TEM (HR-TEM) image of the SnO₂ nanoparticles calcined at 400 °C, for 2 h. It shows clear lattice fringes, indicating the established crystallinity of SnO₂ powders.

For semiconductor materials, the quantum confinement effect is expected if the semiconductor dimension become smaller than the Bohr radius of the exciton, and the absorption edge will be shifted to a higher energy [23]. The room temperature UV–visible spectrum (Fig. 5a) of the as-prepared methanol mediated SnO₂ nanoparticles has the absorption edge is at 312 nm, which is smaller than the band edges observed at 323 and 337 nm for ethanol and water as shown in Fig. 5b, c. In all the cases, blue shifts were observed. Considering the blue shift of the absorption positions from the bulk SnO₂, the absorption onsets of the present samples can be assigned to the direct transition of electron in the SnO₂ nanocrystals. The corresponding band gap energies can be calculated to be 3.97, 3.83 and 3.68 eV and are larger than the bulk SnO₂ [24]. The increasing trends of the band gap energy upon the decreasing particle size are well presented for the quantum confinement effect.

Figure 6 shows the PL spectra of the SnO₂ synthesized in methanol, ethanol and water, which were taken under an excitation wavelength, is 300 nm. High intensity signal in the UV region and low intensity in the visible region in PL spectrum indicate a good surface morphology of SnO₂ nanoparticles. A sharp UV emission peak was observed at 345 nm (Fig. 6a), which attributed to the radiative annihilation of excitons. However, in the case of ethanol and water mediated samples have a weak UV emission peak as in Fig. 6b, c. Two prominent peaks at 467 and 400 nm have been observed in the range 350–500 nm. Particularly, the peak position at 467 nm is sharp and unchanged for all samples whereas its intensity tends to reduce with heat treatment temperature. It is due to the characteristics of the traps present in the nanoparticles [24]. We attribute the emission at 440 nm to electron transition mediated by defects levels in the band gap, such as oxygen vacancies. This is proved by the fact that the temperature behaviour of luminescence spectra of the nanoscaled SnO₂ powders is similar with those from nanocrystals of SrTiO₃, TiO₂, ZnO and BaTiO₃ [25–28]. In the present SnO₂ nanocrystals, the intrinsic defects, such as oxygen vacancies, which act as luminescent centers, can form defect levels located highly

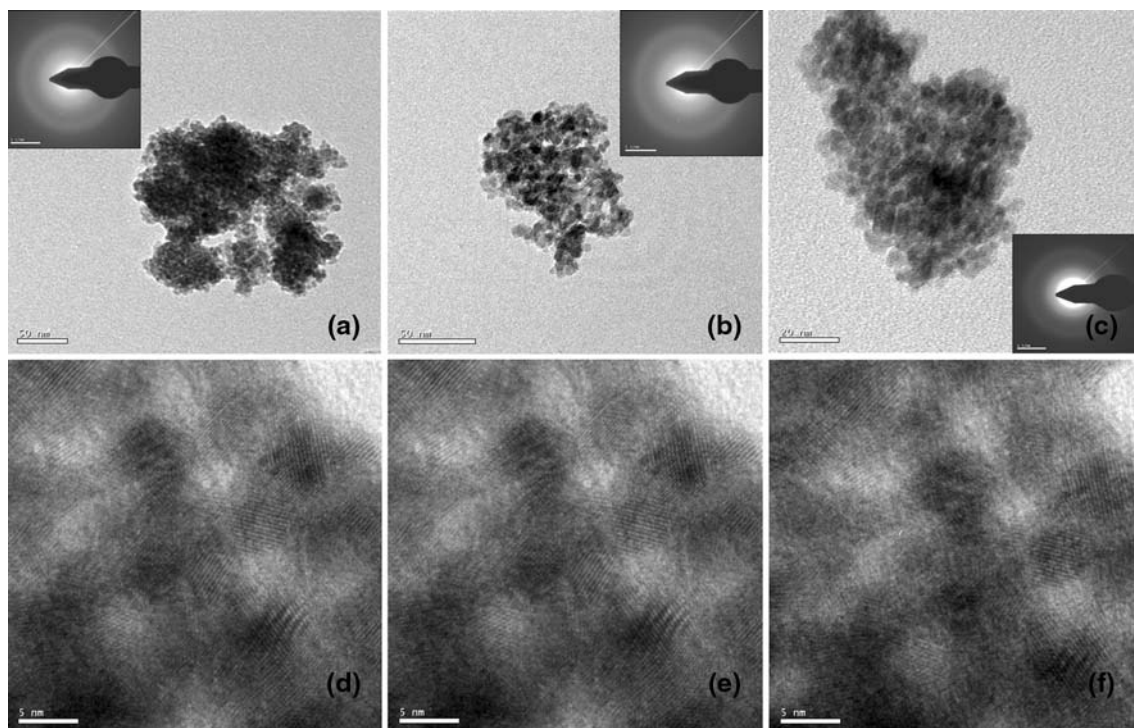


Fig. 4 TEM images of the as-prepared SnO₂ nanoparticles mediated in methanol (a), ethanol (b), and water (c). HR-TEM images of the as-prepared SnO₂ nanoparticles mediated in methanol (d), ethanol (e), and water (f)

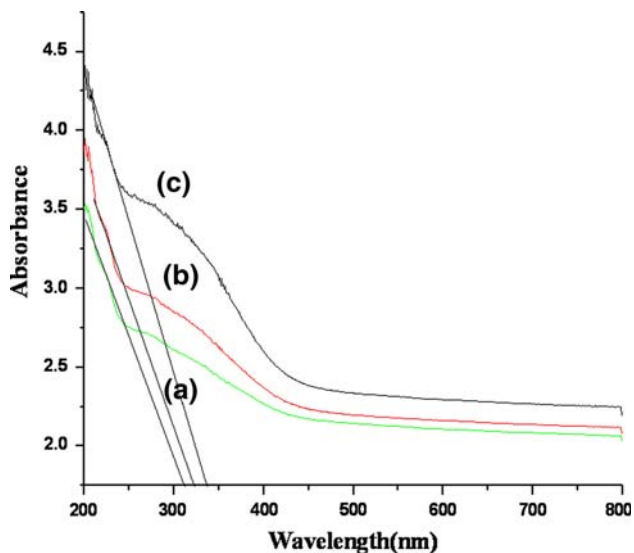


Fig. 5 UV absorption spectra of SnO₂ nanoparticles mediated in methanol (a), ethanol (b), and water (c)

in the gap, trapping electrons from the valence band to contribute to the luminescence.

4 Conclusion

Tetragonal phase methanol, ethanol and water mediated SnO₂ nanoparticles were successfully synthesized using

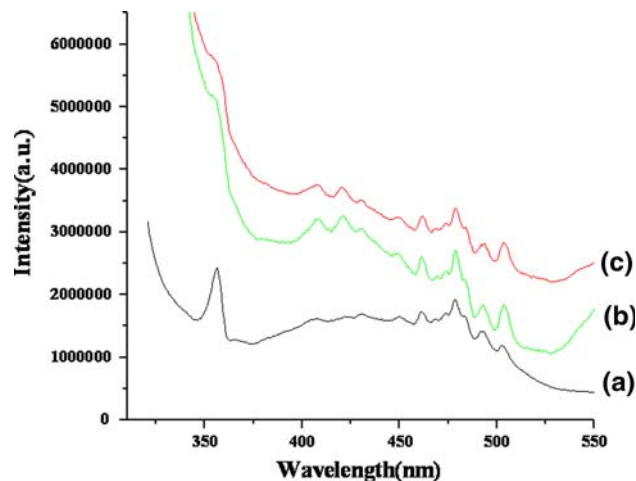


Fig. 6 PL spectra of SnO₂ nanoparticles mediated in methanol (a), ethanol (b), and water (c)

simple sol-gel method. The particle sizes of the SnO₂ nanocrystallites prepared in methanol, ethanol and water were 3.9, 4.5 and 5 nm, respectively, which is conformed by both TEM and XRD results. On the other hand, the morphologies of the as-synthesis SnO₂ nanocrystallites are dependent on the solvent. Considering the blue shift of the absorption positions from the bulk SnO₂, the absorption onsets of the present samples can be assigned to the direct transition of electron in the SnO₂ nanocrystals. In the

present SnO₂ nanocrystals, the intrinsic defects, such as oxygen vacancies, which act as luminescent centers, can form defect levels located highly in the gap, trapping electrons from the valence band to contribute to the luminescence. A spherical like morphology of the prepared methanol mediated SnO₂ nanoparticles was observed in the SEM and TEM studies with size in the range of 3 nm. Considering these results, the preparation of SnO₂ nanoparticles by methanol, it influences the effect of particle size, morphology and optical properties. Moreover, the quantum size SnO₂ nanocrystallites would be promised in the applications of sensor, solar cell and optoelectronic devices.

Acknowledgments The authors are grateful to the University Grant Commission for extending financial support to carryout this work.

References

- Zhang J, Sun L, Pan H, Liao C, Yan C (2002) *New J Chem* 26:33
- Zhang DF, Sun LD, Yin JL, Yan CH (2003) *Adv Mater* 15:1022
- Jorezebsk JM, Marton JP (1976) *J Electrochem Soc* 129:299C
- Baik NS, Sakai G, Miura N, Jamazoe N (2000) *J Am Ceram Soc* 83:2983
- Olivi P, Souza ECP, Longo E, Varela JA, Bulhoes LOS (1993) *J Electrochem Soc* 140:81
- Chopra KL, Major S, Pandya DK (1983) *Thin Solid Films* 102:1
- Tagawa T, Kataoka S, Hattori T, Murakami Y (1994) *Appl Catal* 4:1
- Park PW, Kung HH, Kim DW, Kung MC (1999) *J Catal* 184:440
- Pianaro SA, Bueno PR, Longo E, Varela JA (1995) *J Mater Sci Lett* 14:692
- Bueno PR, Cassia-Santos MR, Leite ER, Longo E, Bisquert J, Garcia-Santiago G (2000) *J Appl Phys* 88:6545
- Bose AC, Kalpana D, Thangadurai P, Ramasamy S (2002) *J Power sources* 107:138
- Chen ZW, lai JKL, Shek CH (2004) *Phys Rev B* 70:165314
- Dieguez A, Rodriguez AR, Vila A, Morante JR (2001) *J Appl Phys* 90:1550
- Arai T (1960) *J Phys Soc Jpn* 15:916
- Jeong J, Choi SP, Chang CI, Shin DC, Park JS, lee BT, Park YJ, Song HJ (2003) *Solid State Commun* 127:595
- Santos LRB, Chartier T, Pagnoux C, Baumard JF, Santilli CV, Pulcinelli SH, Larbot A (2004) *J Eur Ceram Soc* 24:3713
- Grzeta B, Tkalec E, Goebbert C, Takeda M, Takahashi M, Nomura K, Jaksic M (2002) *J Phys Chem Solids* 63:765
- Antonio JAT, Baez RG, Sebastian PJ, Vazquez A (2003) *J Solid state Chem* 174:241
- Zhang J, Gao L (2004) *J Solid State Chem* 177:1425
- Castillo JD, Rodriguez VD, Yanes AC, Ramos JM (2005) *Nanotechnology* 16:S300
- Murray CB, Kagan CR, Bawendi MG (1995) *Science* 270:1335
- Xu J, Tamaki NN, Yamazoe N (1991) *Sens Actuators B* 3:147
- Wang Y, Herron N (1991) *J Phys Chem* 95:525
- Ningthoujam RS, Kulshreshtha SK (2008) *J Mat Res Bull* 6:4147
- Zhang WF, Yin Z, Zhang MS, Du ZL, Chen WC (1999) *J Phys Cond Mat* 11:5655
- Zhang WF, Zhang MS, Yin Z, Chen Q (2000) *Appl Phys B* 70:261
- Zhang WF, Zhang MS, Yin Z (2000) *Phys Stat Solid A* 179:319
- Bahnemann DW, Kormann C, Hoffmann MR (1987) *J Phys Chem* 91:3789